

Fully Integrated Microfluidic Platform Enabling Automated Phosphoprofiling of Macrophage Response

Nimisha Srivastava,^{*,†} James S. Brennan, Ronald F. Renzi, Meiyie Wu, Steven S. Branda, Anup K. Singh, and Amy E. Herr[‡]

Sandia National Laboratories, 7011 East Avenue, Livermore, California 94550

The ability to monitor cell signaling events is crucial to the understanding of immune defense against invading pathogens. Conventional analytical techniques such as flow cytometry, microscopy, and Western blot are powerful tools for signaling studies. Nevertheless, each approach is currently stand-alone and limited by multiple time-consuming and labor-intensive steps. In addition, these techniques do not provide correlated signaling information on total intracellular protein abundance and subcellular protein localization. We report on a novel phosphoFlow Chip (pFC) that relies on monolithic microfluidic technology to rapidly conduct signaling studies. The pFC platform integrates cell stimulation and preparation, microscopy, and subsequent flow cytometry. pFC allows host-pathogen phosphoprofiling in 30 min with an order of magnitude reduction in the consumption of reagents. For pFC validation, we monitor the mitogen-activated protein kinases ERK1/2 and p38 in response to *Escherichia coli* lipopolysaccharide (LPS) stimulation of murine macrophage cells (RAW 264.7). pFC permits ERK1/2 phosphorylation monitoring starting at 5 s after LPS stimulation, with phosphorylation observed at 5 min. In addition, ERK1/2 phosphorylation is correlated with subsequent recruitment into the nucleus, as observed from fluorescence microscopy performed on cells upstream of flow cytometric analysis. The fully integrated cell handling has the added advantage of reduced cell aggregation and cell loss, with no detectable cell activation. The pFC approach is a step toward unified, automated infrastructure for high-throughput systems biology.

Innate immune response encompasses an ensemble of cellular-level events.¹ Phosphorylation and subsequent dephosphorylation of intracellular proteins are transitory events that play a pivotal role in signaling cascades. Importantly, measurement of inherently rapid and transitory signaling events can shed light on the timing and degree of immune response to stimulation. Nevertheless until the recent advent of fluorescent reagents for phospho-epitope

staining, assays offered limited and static snapshots of signaling.^{2,3} Phospho-staining combined with flow cytometry supplies single-cell measurements required to tease apart stochastic variation within large heterogeneous cell populations.^{4,5} While flow cytometers offer high-throughput (1000 cells/s) multiparametric (up to 17 parameters) detection, the multiple sample preparation and handling steps required (i.e., stimulation, fixation, permeabilization, antibody staining, washing) are labor intensive, inefficient, time-consuming and can require large, expensive instrumentation. In addition, fine temporal information is difficult to obtain using manual, benchtop handling (i.e., Petri dishes, centrifuge tubes). Benchtop methods make reproducible measurement of fleeting phosphorylation events difficult. Consequently, integration of upstream cell preparation with subsequent flow cytometry has striking relevance to phospho-profiling studies.

Recent strides in instrumentation and high-throughput sample preparation (i.e., 96 well plates, liquid autosamplers) have yielded phosphorylation data for large sample sets.⁶ Measurement technology capable of monitoring phosphorylation with fine temporal resolution and hands-free operation would further advance signaling studies. Chief among the advantages of microfluidic analytical systems is the integration of preparation and analysis and the ensuing capability for automation. Microfluidic tools have been demonstrated primarily for individual functions including flow cytometry^{7–10} and fluorescence-activated cell sorting,^{11–13} as well as cell culture,^{14–17} surface patterning,¹⁸ rapid stimulation,¹⁹ and

- (2) Weijer, C. J. *Science* **2003**, *300*, 96–100.
- (3) Zorov, D. B.; Kobrinsky, E.; Juhaszova, M.; Sollott, S. J. *Circ. Res.* **2004**, *95*, 239–252.
- (4) Perez, O. D.; Nolan, G. P. *Nat. Biotechnol.* **2002**, *20*, 155–162.
- (5) Sachs, K.; Perez, O.; Pe'er, D.; Lauffenburger, D. A.; Nolan, G. P. *Science* **2005**, *308*, 523–529.
- (6) www.bdbiosciences.com, www.amnis.com, www.beckmancoulter.com.
- (7) Huh, D.; Gu, W.; Kamotani, Y.; Grotberg, J. B.; Takayama, S. *Physiol. Meas.* **2005**, *26*, R73–R98.
- (8) Simonnet, C.; Groisman, A. *Anal. Chem.* **2006**, *78*, 5653–5663.
- (9) Palkova, Z.; Vachova, L.; Valer, M.; Preckel, T. *Cytometry, Part A* **2004**, *59A*, 246–253.
- (10) Chan, S. D. H.; Luedke, G.; Valer, M.; Buhlmann, C.; Preckel, T. *Cytometry, Part A* **2003**, *55A*, 119–125.
- (11) Fu, A. Y.; Spence, C.; Scherer, A.; Arnold, F. H.; Quake, S. R. *Nat. Biotechnol.* **1999**, *17*, 1109–1111.
- (12) Wang, M. M.; Tu, E.; Raymond, D. E.; Yang, J. M.; Zhang, H. C.; Hagen, N.; Dees, B.; Mercer, E. M.; Forster, A. H.; Kariv, I.; Marchand, P. J.; Butler, W. F. *Nat. Biotechnol.* **2005**, *23*, 83–87.
- (13) Perroud, T. D.; Kaiser, J. N.; Sy, J. C.; Lane, T. W.; Branda, C. S.; Singh, A. K.; Patel, K. D. *Anal. Chem.* **2008**, *80*, 6365–6372.
- (14) Gomez-Sjoberg, R.; Leyrat, A. A.; Pirone, D. M.; Chen, C. S.; Quake, S. R. *Anal. Chem.* **2007**, *79*, 8557–8563.

* Corresponding author. E-mail: srivastava.nimisha@gmail.com.

[†] Currently at Department of Mechanical Engineering, University of California, Santa Barbara, CA 93106.

[‡] Currently at Department of Bioengineering, University of California, Berkeley, CA 94720.

(1) Lipniacki, T.; Paszek, P.; Brasier, A. R.; Luxon, B. A.; Kimmel, M. *Biophys. J.* **2006**, *90*, 725–742.

single cell arrays.^{20,21} We see promise in ready microfluidic integration of unit functions, both preparatory and analytical, to form the basis for a coherent tool optimized to characterize signaling at the single-cell level. Particularly advantageous for monitoring numerous time points in a large experimental parameter space needed for signaling studies,^{22–24} a monolithic preparation and measurement platform would allow programmable control of time point selection, both for dosing of challenge and measurement of response.

We report on the design and experimental validation of a microfluidic platform that incorporates and automates all preparatory and analytical steps necessary for phospho-profiling of both adherent and nonadherent cells. A murine macrophage cell line (RAW 264.7) with lipopolysaccharide (LPS) challenge was chosen for pFC validation. The endotoxin LPS is a major component of Gram-negative pathogenic bacteria (e.g., *Yersinia pestis* and *Francisella tularensis*) and induces activation of macrophages through Toll-like receptors (TLR4).^{25,26} Upon activation, TLR4 triggers a signaling cascade that includes phosphorylation of protein kinases ERK and p38.²⁷ This cascade induces the expression of immune activation genes that steer the course for immediate defense against pathogen invasion. Such immediate molecular events associated with innate immune response are categorized as “first responders” and typically occur in the first few seconds to minutes after stimulation and, inherently, necessitate fine temporal resolution.

We apply the pFC platform to monitor the phosphorylation of two key proteins in the TLR4 pathway: extracellular signal-regulated kinase (ERK1/2) and p38. Pressure-driven flow in microfluidic devices is programmed to automate the following process steps: (1) LPS challenge of macrophage cells which includes dosing, rapid mixing, and timed incubations, (2) all phospho-profiling preparatory steps, namely, macrophage fixation, plasma membrane permeabilization, fluorescence immuno-staining, and numerous intermediate washing steps, and (3) subsequent flow cytometry. In addition, the pFC platform is compatible with fluorescence microscopy, thus enabling real-time observation of cell phenotype prior to flow cytometry.

MATERIALS AND METHODS

Cell Culture and Phosphorylation Assays. The RAW 264.7 murine macrophage cell line was purchased from ATCC (Manassas, VA) and was used for all studies. Macrophages were cultured

- (15) Petronis, S.; Stangegaard, M.; Christensen, C. B. V.; Dufva, M. *Biotechniques* **2006**, *40*, 368–376.
- (16) Zhu, X. Y.; Chu, L. Y.; Chueh, B. H.; Shen, M. W.; Hazarika, B.; Phadke, N.; Takayama, S. *Analyst* **2004**, *129*, 1026–1031.
- (17) Gu, W.; Zhu, X.; Futai, N.; Cho, B. S.; Takayama, S. *Proc. Natl. Acad. Sci. U.S.A.* **2004**, *101*, 15861–15866.
- (18) Abhyankar, V. V.; Beebe, D. J. *Anal. Chem.* **2007**, *79*, 4066–4073.
- (19) El-Ali, J.; Gaudet, S.; Gunther, A.; Sorger, P. K.; Jensen, K. F. *Anal. Chem.* **2005**, *77*, 3629–3636.
- (20) Wang, Z. H.; Kim, M. C.; Marquez, M.; Thorsen, T. *Lab Chip* **2007**, *7*, 740–745.
- (21) King, K. R.; Wang, S. H.; Irimia, D.; Jayaraman, A.; Toner, M.; Yarmush, M. L. *Lab Chip* **2007**, *7*, 77–85.
- (22) El-Ali, J.; Sorger, P. K.; Jensen, K. F. *Nature* **2006**, *442*, 403–411.
- (23) Sims, C. E.; Allbritton, N. L. *Lab Chip* **2007**, *7*, 423–440.
- (24) Rosenbluth, M. J.; Lam, W. A.; Fletcher, D. A. *Lab Chip* **2008**, *8*, 1062–1070.
- (25) Takeda, K.; Kaisho, T.; Akira, S. *Annu. Rev. Immunol.* **2003**, *21*, 335–376.
- (26) Akira, S.; Takeda, K. *Nat. Rev. Immunol.* **2004**, *4*, 499–511.
- (27) Banerjee, A.; Gerondakis, S. *Immunol. Cell Biol.* **2007**, *85*, 420–424.

in growth medium consisting of 450 mL of DMEM, 50 mL of FBS (gemcell), 5 mL of HEPES, 5 mL of L-glutamine (200 mM), and 1:100 penicillin/streptomycin. A 5×10^6 cells/mL cell suspension was used to load cells on the chip. All on-chip assays were validated with conventional benchtop setups and analysis using a BD FACScan flow cytometer (BD Biosciences, San Jose, CA). For these benchtop assays, macrophage cells were challenged with smooth *Escherichia coli* LPS (Sigma-Aldrich, St. Louis, MO) inside an incubator (37 °C, 5% CO₂). At various predetermined incubation time points (i.e., 5 s, 15 min, 30 min, 60 min), the LPS challenged macrophage cells were fixed (temporally and spatially) using 2% paraformaldehyde (Electron Microscopy Sciences, Hatfield, PA) at room temperature for 10 min, washed, permeabilized with 100% methanol (Electron Microscopy Sciences) at 4 °C for 20 min, washed and labeled with fluorescently tagged phospho-specific antibodies (ERK, Cell Signaling Technology, Inc. (Danvers, MA) catalog no. 4374; p38, BD Biosciences, catalog no. 612594; JNK, Abcam (Cambridge, MA), catalog no. 47337) for 20 min at RT. After two more washes, the labeled cells were analyzed on a FACScan equipped with a 488 nm argon ion laser and three detection channels (FL1-green, FL2-yellow, and FL3-red). Washing was performed by forming a pellet of cells using centrifugation at 400g for 5 min with pellet resuspension using a phosphate-buffered saline (pH 7.4) solution.

Microfluidic Platform. Chip designs were made in-house using AutoCAD 2000 (Autodesk Inc., San Rafael, CA), photomasks were generated at Photo Sciences (Torrence, CA), and quartz microfluidic devices were fabricated by Caliper Life Sciences (Hopkinton, MA). Care was taken during chip design and plumbing to minimize dead volume. An array of eight holes (500 μm diameter) provided for fluid inlet. Fluidic connection to the inlet holes was made using an in-house designed plastic (Delrin) manifold and PEEK tubing (125 μm i.d., 1/32 in o.d., Upchurch Scientific (Oak Harbor, WA)). The small i.d. of the PEEK tubing (125 μm) allowed for low residence time during reagent and cell delivery, which was critical in reducing cell loss by axial dispersion in the tubing. An in-house designed shut-off electronic valve (response time <1 s, dead volume ~20 nL) was used in-line with the PEEK tubing. On the other end, PEEK tubing was immersed in an airtight sample/reagent reservoir. The reservoir was pressurized using house nitrogen and electronic pressure controllers (Parker Hannifin, Cleveland, OH) to load sample/reagent into the chip. Typically pressures ranging from 0.2 to 5 psi were used during device operation. Higher pressures, up to 15 psi, were used if necessary to remove bubbles and during cleaning cycles. Each quartz chip could be used repeatedly with an appropriate cleaning protocol (Supporting Information). The microfluidic channels and inlet wells were filled with DI water prior to making the fluidic connections.

Temperature Control on the pFC Platform. The pFC platform was mounted on a thermal control setup to achieve the desired temperature regulation during cell culture and stimulation. The thermal control setup consisted of a thermoelectric hot plate (TE Technology Inc., Traverse City, MI) and a proportional integral controller. A temperature sensing thermistor was attached to the quartz chip to provide temperature feedback to the controller. The setup was capable of maintaining temperatures from 0 to 100 °C with an accuracy of ±0.1 °C.

Photolithographic Fabrication of Porous Polymer Filters.

Butyl methacrylate monomer (Sigma-Aldrich, St. Louis, MO) was treated with activated basic alumina to remove the manufacturer added inhibitor. After treatment butyl methacrylate was added to 1,3-butanediol diacrylate (BDDA, Sigma-Aldrich) to achieve a 60:40 ratio. The AIBN (azobisisobutyronitrile) photoinitiator was added to the monomer solution to achieve a 0.3 wt % of photoinitiator and mixed by sonication for 1 min. (Caution: Do not over sonicate, as heating can initiate polymerization.) The casting solvent was made by adding 1,4-butanediol (J.T. Baker, Phillipsburg, NJ), DI water, and 1-propanol (Sigma-Aldrich) in that order to achieve a 28:10:62 ratio. The monomer mixture was added to the casting solvent in a 40:60 ratio and vortexed for 30 s. Aliquots were stored at -20 °C for up to 1 week. (Caution: Because of the presence of volatile components, the composition of the formulation may change with each degassing and purging cycle.) Prior to porous filter fabrication, the quartz channel surfaces were treated with silane, as described elsewhere.²⁸ The polymer precursor solution was sonicated and degassed for 10 min followed by a N₂ purge for 5 min. After silane treatment, channels were washed with ethanol for ~10 min. Note the ethanol wash step is extremely critical, any residual silane treatment will prevent acrylate polymerization. A N₂ purge of ~5 min was used to dry the channels. The polymer precursor solution was wicked into the chip via capillary action. All the ports were filled with precursor solution to prevent pressure driven flow in the chip. The identified region of the chip was exposed to a 355 nm laser excitation (Teem Photonics, Wellesley, MA) until a white monolith was detectable, typically 2 min, with an additional 2 min exposure. After monolith fabrication, excess precursor solution was removed using vacuum. Channels were washed with ethanol as described above and stored hydrated at 4 °C until use.

Polyethylene Glycol (PEG) Photograft Preparation. The quartz channels were first covalently coated with a monolayer of silane, as described elsewhere.²⁸ The precursor solution for preparing the PEG graft consisted of 3% PEG-acrylate (Sigma-Aldrich, MW 300) in DI water with 0.5% V50 photoinitiator (Wako Specialty Chemicals, Richmond, VA). The precursor solution was degassed for 10 min. The microfluidic channels were purged and dried with N₂ for 10 min, before adding the precursor solution. The chip was then exposed to a high voltage UV lamp (100 W) for 15 min. A circulating fan kept the chip at room temperature. After the 15 min UV exposure, the chip was flushed with water for 10 min and stored hydrated and refrigerated until use. After each use, pFC was cleaned and recoated with the PEG photograft.

Single Point Fluorescence Detection for On-Chip Flow Cytometry. The pFC detector was developed to emulate the capabilities of conventional flow cytometry detection. An air-cooled 15 mW argon ion laser (Melles Griot, Albuquerque, NM) with a single wavelength emission at 488 nm was used for excitation. The optical train consisted of a series of adjustable mirrors and a 60× air objective for epi-fluorescence illumination through which the laser beam was introduced to the on-chip detection window.

The microfluidic device was aligned with precise 3-axis control (Supplemental Figure 4 in the Supporting Information).

The emitted light from the hydrodynamically focused stream of cells was collected through two fluorescence filter cubes with a dichroic mirror (505 DRLP green and 650 DRLP red, Omega Optical, Inc., Brattleboro, VT) and associated emission filters (535 AF45 green, 695 AF55 red). The collected light from each filter cube was relayed to two Hamamatsu photomultiplier tubes (PMTs), and the PMT gain was tuned using a Hamamatsu H5784 PMT interface/controller. In addition, the scatter signal from an optical fiber positioned on the top surface of the quartz device was relayed to a third Hamamatsu PMT. The real-time signal from the PMT was collected using a computer equipped with National Instruments CompactRIO programmable automation controller.

The data was further analyzed using the Peak Finder application in LabVIEW (National Instruments, Austin, TX) to construct population histograms of time-resolved phosphorylation assays. The Peak Finder program uses the LabVIEW Peak Fit routine to fit the peak of the raw signal traces from the PMT with a polynomial fit returning the peak amplitude and width. A model Gaussian peak was then computed and overlaid for each peak in the raw trace for visual validation. Once the fit parameters were optimized, the amplitudes of the peak were used to display histograms in Matlab (MathWorks, Inc., Natick, MA).

Microscopy and Image Analysis. Bright field, epi-fluorescence and phase contrast images were captured at 10× and 40× magnification on an Olympus IX-71 inverted microscope equipped with a CoolSNAP HQ CCD camera (Photometrics, Tucson, AZ) and Image-Pro software (Media Cybernetics, Bethesda, MD). To measure the aggregation index for on-chip and off-chip cells, images were further analyzed using ImageJ.²⁹ The image processing algorithm utilized background subtraction (rolling ball radius = 50, with white background unchecked), setting lower and upper levels on the threshold to convert to a binary image, and finally analyzing the particles based on size and circularity to show outlines for single cells and for aggregates. The “Analyze Particles” plug-in in ImageJ was used to measure the number of single cells and aggregates.

RESULTS

The pFC platform consists of a planar microfluidic chip coupled with flow control hardware attached to an epi-fluorescence microscope allowing full-field and single-point fluorescence detection (Figure 1). To provide a versatile platform, the pFC tool has two operating modes for the analysis of adherent and nonadherent cell types. Both operating modes required nominal user intervention, as programmable flow controllers and valves automated the multiple steps required for phospho-profiling. Here we demonstrate the pFC approach to automate sequential introduction of multiple reagents required for cell signaling studies, including cell introduction, cell infection, phospho-epitope staining,³⁰ and finally imaging and flow cytometry (Figure 1). The pFC device consists of a microfluidic network that includes two wide spiral incubation chambers. Each chamber holds ~2000 cells per assay and 350 nL of fluid volume. We have observed that a spiral geometry

(28) Ngola, S. M.; Fintschenko, Y.; Choi, W. Y.; Sheppard, T. J. *Anal. Chem.* 2001, 73, 849–856.

(29) Abramoff, M. D.; Magalhaes, P. J.; Ram, S. J. *Biophoton. Int.* 2004, 11, 36–41.
(30) Krutzik, P. O.; Nolan, G. P. *Cytometry, Part A* 2003, 55A, 61–70.

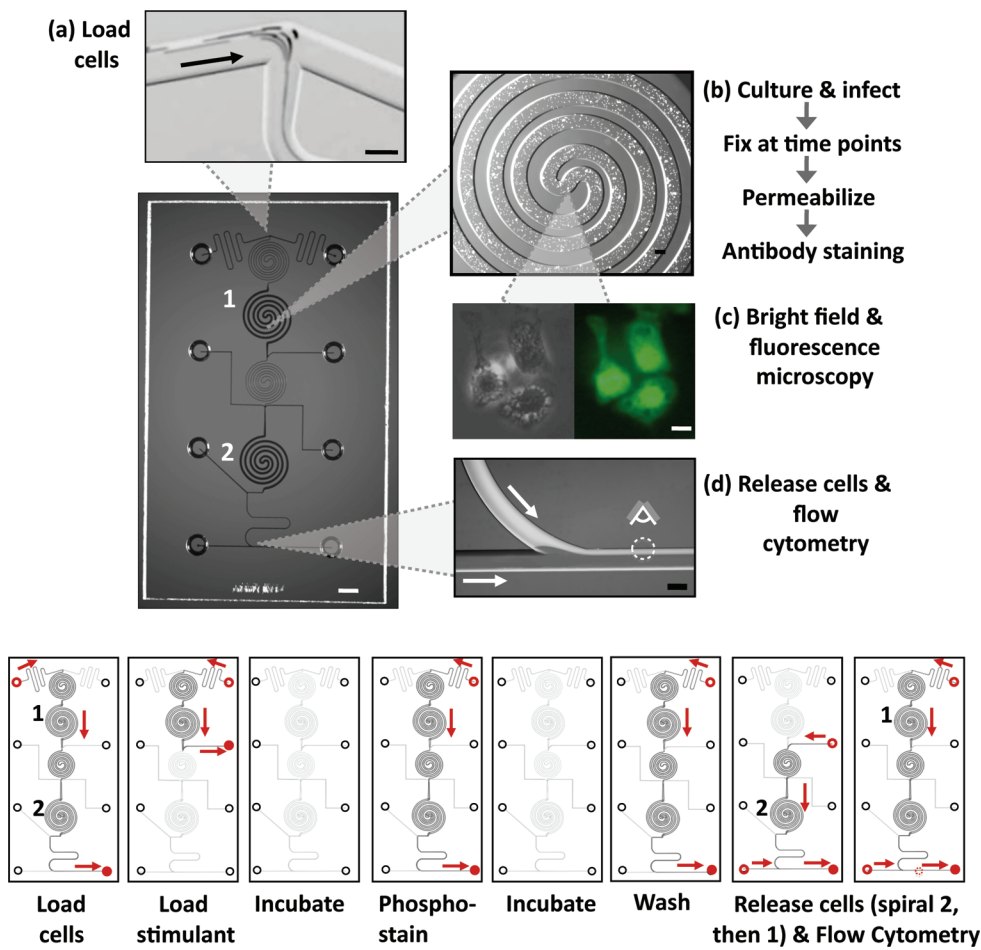


Figure 1. pFC enables streamlined, automated phospho-profiling of macrophage response to LPS on a microfluidic platform. (top panel) pFC device for phospho-profiling of adherent cells. Device operation proceeds from top to bottom. The two wide spirals (1 and 2) enable simultaneous infection and control assay. (a) Macrophage cells are introduced into the pFC via pressure-driven flow, (b) incubation chambers (wide spirals, only one of the two is shown) where the automated pFC phosphorylation assay proceeds as (1) cell culture and infection, (2) phospho-profiling (fixation, permeabilization, and staining with phospho-specific antibodies), (c) imaging, and (d) flow cytometry. Scale bars: 2 mm (chip image), 100 μm (a, d), 200 μm (b), and 10 μm (c). (bottom panel) Detailed step-by-step operation of the pFC platform, from loading cells to end-point detection by flow cytometry. Red arrows indicate the direction of flow, highlighted wells indicate external fluid valve to that inlet well is open (all others being closed), channels in dark gray support continuous flow while regions in light gray contain stagnant flow.

minimizes dead volume and associated carry-over of stagnant fluid during fluid exchange. The wide channel incubation chambers are fluidically isolated from each other through high fluidic resistance (narrow width) spiral features. Timed continuous and stopped flow intervals facilitate multistep reagent delivery and incubation protocols.

pFC for Analysis of Adherent Cells. To study signaling in adherent cells, a sequence of processing steps was employed. The phospho-profiling workflow progressed in a unidirectional manner from the top of the pFC device to the bottom of the chip (Figure 1). Dual spiral incubation chambers allowed concurrent execution of a control assay with a challenge assay. The pFC phospho-profiling assay was initiated by pressure-driven delivery of a cell suspension from off-chip reservoirs into the chip (supplemental movie “Seeding of the pFC with macrophages” in the Supporting Information). During the loading step, the microfluidic incubation chambers were visually assessed to ensure complete cell seeding. Once the incubation chambers were populated with cells, the loading flow was stopped and cells were observed as they settled to the incubation chamber floor.

The cell settling time was approximated using the settling velocity (v) for cells in a dilute suspension using $v = (\rho/\mu)r^2(\Delta\rho)g/\mu$, where $\Delta\rho$ is the deviation of the density of macrophages from that of the media, μ is the viscosity of the media, r is the average size of a macrophage (10 μm), and g is the gravitational force. Density gradient centrifugation yields a ρ of 1.05 g/mL for macrophage cells. For the media, ρ is 1.01 g/mL. Although the required settling time was <1 s, a conservative 5 min settling interval was used to ensure that the macrophage cells had not only settled but were also firmly attached to the channel floor. Subsequent shear flow assays suggest that macrophage cell adhesion to the quartz channel floor exceeded 1.7 nN, the maximum force available from the highest accessible volumetric flow rate of 50 $\mu\text{L}/\text{min}$ (Supplemental Figure 1a in the Supporting Information).

After cells were immobilized on the channel floor, exogenous stimulation was initiated by flowing LPS through the first spiral incubation chamber (Figure 1). The second chamber (Figure 1a, spiral marked 2) was used for negative control assays (no LPS). The stimulation duration in spiral 1 was controlled by a precise

interval of stopped flow. The low volume of the incubation chamber ($V = 350$ nL) coupled with applied flow rates ($Q = 5 \mu\text{L}/\text{min}$) enabled rapid fluid exchange ($t = V/Q = 4$ s) that in turn facilitated short stimulations, thus allowing studies of early signaling (Supplemental Figure 1b in the Supporting Information). After a timed LPS challenge, a chemical fixative (2% paraformaldehyde) was introduced into both spiral incubation chambers. After fixation, the two spiral chambers were flushed with methanol to permeabilize cell membranes. Numerous programmed intermediate buffer exchanges were subsequently conducted to limit cross-contamination. Post permeabilization, the cells were incubated with fluorescently tagged phospho-specific antibodies to label the phosphorylated epitopes of p38 and ERK1/2.

After phospho-staining, the immobilized cells in the pFC incubation chambers were investigated using epi-fluorescence and bright-field microscopy (Figure 1b). With the use of visual microscopy inspection (Figure 1c), intracellular localization of phosphorylated ERK1/2 and p38 was observed in LPS challenged cells (spiral chamber 1). Localization was characterized by high fluorescence signal centralized to the nucleus of the cell, identified through companion DIC microscopy. No phosphorylation of ERK1/2 or p38 was detectable via fluorescence microscopy in the negative control assay (spiral chamber 2). After imaging, the immobilized cells were released from the floor of the incubation chambers using a high flow rate purge of the chambers with a trypsin-containing buffer (supplemental movie “Enzymatic cell removal” in the Supporting Information). The cell suspension was hydrodynamically focused and on-chip flow cytometry performed (supplemental movie “Hydrodynamic Focusing” in the Supporting Information). A 10:1 focusing of the sample flow enabled throughput (100 cells/min) comparable to other reported on-chip flow cytometry analyses. Less than 10 μL of sample volume was necessary to complete the reported analysis, roughly 0.1% of the volume required for conventional flow cytometry. The magnitude of the fluorescence signal detected by the flow cytometer PMT's was used to establish the degree of protein phosphorylation in each cell detected, as described later in the section regarding TLR4 signaling. For validation purposes, released cells were collected from the waste reservoir and analyzed via conventional flow cytometry.

pFC for Analysis of Nonadherent Cells. While our studies of LPS-mediated activation of innate immunity and subsequent protein phosphorylation relied on a RAW 264.7 cell model that was adherent, design modifications to the pFC platform allowed ready analysis of nonadherent cell types (Figure 2). Here we demonstrate operation of the pFC platform for analysis of macrophage cells without allowing cell attachment to the floor of the pFC device (Figure 2a). To demonstrate the feasibility of the analysis of nonadherent cells, unlike macrophages which are adherent, two design modifications were employed (1) the polyethylene glycol (PEG) surface graft treatment was used to prevent macrophage cells from adhering to the pFC quartz channel floors even under quiescent conditions. This helped simulate the scenario of phospho-profiling nonadherent cell types. (2) In situ photopolymerized porous monoliths were fabricated on a side channel that acted as a size-exclusion filter, thus allowing bulk pressure-driven fluid flow while retaining and localizing nonadherent, suspended cells at the filter

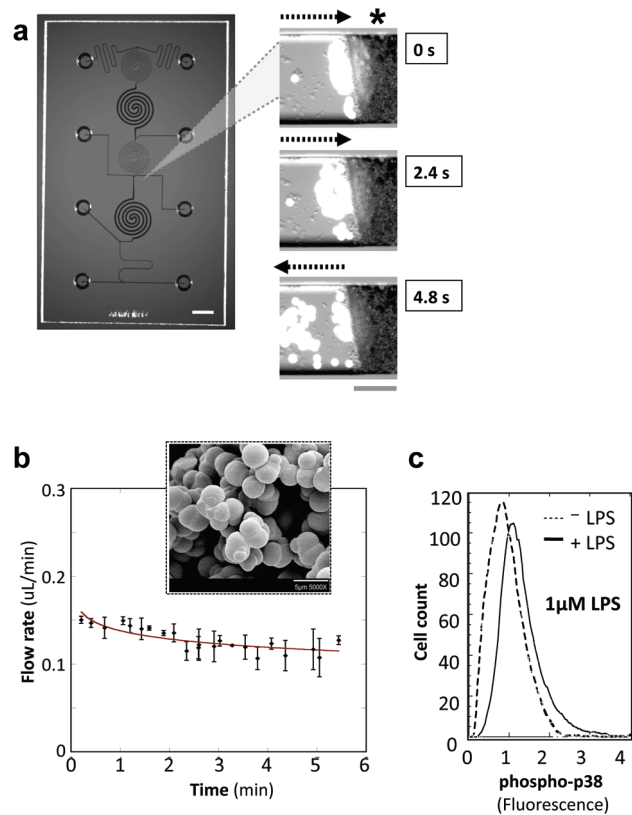


Figure 2. pFC technique for phospho-profiling of nonadherent cell phenotypes. Inclusion of PEG grafted quartz channel surface and in situ photopolymerized porous filter allow capture, washing, and analysis of nonadherent cells on the pFC microfluidic platform. (a) Fluorescence images illustrate rapid fluorescent bead capture and washing using an on-chip polymer filter. The width of the filter is the same as that of the side channel (90 μm) and is 250 μm long. The length of the polymer filter is defined by adjusting the waist of the focused laser beam. Dashed arrows indicate the direction of fluid flow, the scale bar is 50 μm , and the filter is marked with an asterisk. (b) The fluid flow rate through the porous filter remains uniform even as cells collect and concentrate at the interface during washing and buffer exchange. (inset) Scanning electron micrograph of a porous filter with a pore size of $\sim 4 \mu\text{m}$. (c) Phosphorylation of p38 reveals the nonadherent phenotype response of RAW 264.7 macrophage cells to 30 min of stimulation with LPS at 37 °C. Flow cytometry was performed on-chip. For comparison, basal levels of phosphorylated p38 (with no LPS) are also shown.

interface. The width of the filter was the same as that of the side channel (90 μm), and their length was 250 μm .

The polymer filter was fabricated using phase-separation photopolymerization optimized to achieve a pore-size of 4 μm diameter.²⁸ To initiate buffer exchange, vacuum (~17 kPa) was applied downstream of the polymer filter to draw cells to the polymer filter interface (Supporting Information). Since the pore-size is smaller than the size of a cell (~10 μm), cells stacked up at the filter interface while the surrounding liquid was driven through the pores at flow rates of ~ 100 nL/min. The flow rate of liquid through the filter was observed to be stable even as hundreds of cells collected at the filter interface (Figure 2b). Once exchange of reagent was complete, cells were released from the filter interface using a brief pressure pulse of ~ 100 kPa for 1 s. The collection/release operation was repeated for each reagent/buffer exchange step. Only one photopolymerized filter was sufficient for all washes and reagent exchanges. To test the

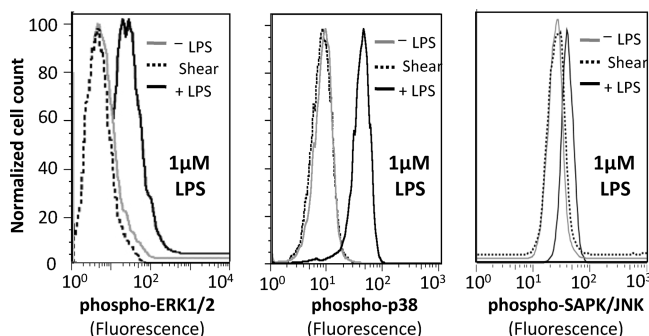


Figure 3. Analysis of phosphorylation for three key intracellular signaling proteins: ERK1/2, stress sensitive p38, and SAPK/JNK, suggesting no signaling artifacts arising from shear stress generated via pFC-mediated microfluidic cell handling. The maximum volumetric flow rate used for the phospho-profiling assay was limited to 5 $\mu\text{L}/\text{min}$. Cells were collected after flowing through the pFC at 5 $\mu\text{L}/\text{min}$, fixed with 2% paraformaldehyde in the outlet reservoir, phospho-stained, and analyzed on BD FACscan.

phospho-profiling protocol using the pFC for analysis of nonadherent cell phenotypes, we employed the modified pFC device design to measure p38 phosphorylation in response to a 1 μM LPS challenge of 30 min duration (Figure 2c). As expected, use of the pFC tool for challenge, preparation, and on-chip flow cytometry of the nonadherent cell phenotype showed increased levels of phospho-p38 measurable in the challenged population, as compared to the negative control.

Effect of Shear Rate Mediated Activation on Macrophage Cells. To assess that shear rates generated during pFC handling of cells did not lead to macrophage activation, we measured phosphorylation of three proteins in the MAPK pathway, ERK1/2, p38, and JNK after pFC handling. Phosphorylation of the latter two proteins is known to be indicative of environmental stresses on the cell.³¹ JNK is also called a Stress-Activated Protein Kinase (SAPK). For comparison, we considered both positive (30 min challenge of 1 μM LPS) and negative controls (no LPS). To test the effect of shear rates, macrophage cells were flowed through the pFC device at the maximum operational shear rate (3000 s^{-1}) and collected in the downstream off-chip reservoir. These cells were then stained with phospho-specific antibodies against ERK1/2, p38, and JNK. Gold-standard flow cytometry of cells subjected to pFC handling showed no detectable phosphorylation for either of the three target proteins (Figure 3). Cells challenged with 1 μM LPS (positive control) under identical handling conditions showed appreciable phosphorylation of ERK1/2 and p38, with lesser response from SAPK/JNK as anticipated.

pFC Allows Improved Handling of Cells. To characterize cell loss and the aggregation tendency of adherent cells during and after pFC phospho-profiling, we assessed the singlet versus aggregate state of RAW 264.7 cells at various points during the pFC manipulation. Microscopy-based inspection of the incubation chambers prior to stimulation, after LPS stimulation (Figure 4a), and after all subsequent phospho-staining steps revealed negligible cell loss. After trypsin release, we observed no retained macrophage cells in the incubation chambers, indicating no cell loss during flow cytometry. In contrast, benchtop preparation resulted in a

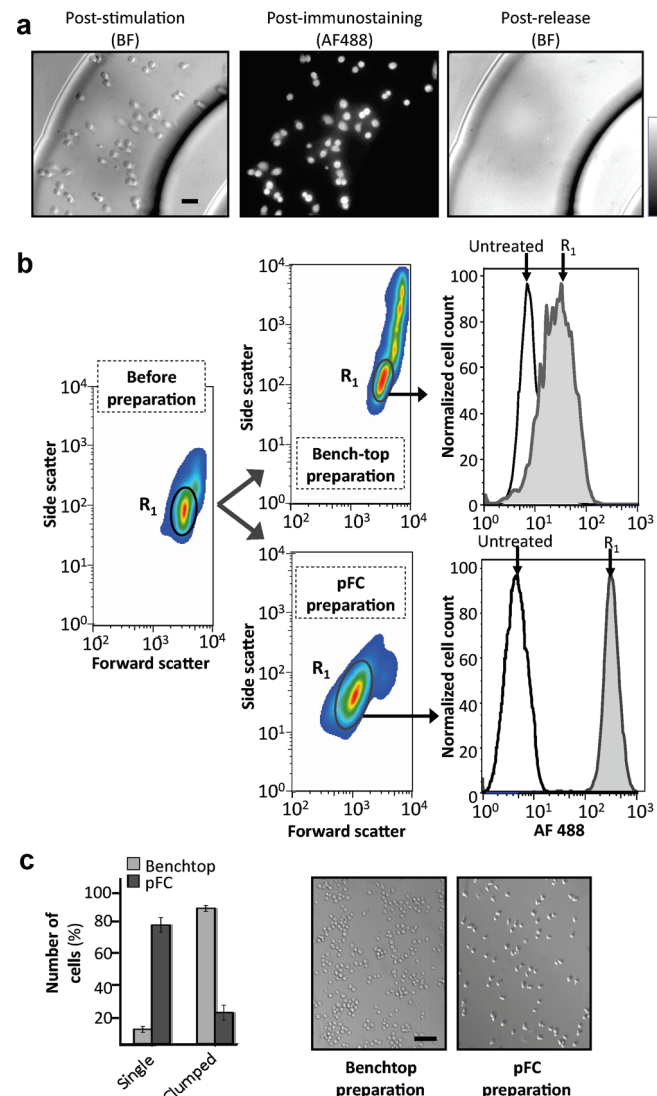


Figure 4. pFC enables high-quality cell preparation via well-controlled cell handling. (a) Bright field (BF) and fluorescence images of macrophage cells in spiral incubation chamber after LPS stimulation, after phospho-staining, and after trypsin release. Cells are well-spread and confined to the incubation chamber with minimal cell release until addressed with trypsin. Scale bar, 20 μm . (b) FACScan side and forward scatter density plots reveal that 70 \pm 9% of cells prepared using the pFC tool were present as single cells (R₁) compared to 45 \pm 6% from conventional preparation ($n = 8$). Error denotes a 96% confidence interval. Cells in region R₁ have a higher coefficient of variation when prepared using benchtop protocols (CV = 46%) as compared to pFC prepared cells (CV = 29%). (c) Bright field analysis of prepared cells confirm a lower aggregation index (0.17 vs 0.91) for pFC prepared cells as compared to standard benchtop preparation. Bright field images confirm qualitative aggregation behavior. The initial cell density for pFC as well as benchtop preparation was 5 \times 10⁶ cells/mL. Scale bar is 100 μm .

total loss of \sim 75% of cells as measured by hemocytometry. The centrifugation-based washing steps were found to contribute substantially to the losses identified in the benchtop method. Such excessive losses (\sim 75%) are usual in protocols that involve chemical permeabilization of the cell membrane as required in phospho-profiling.

We also tested the impact of pFC manipulation on the generation of debris and large cell aggregates, as compared to benchtop preparation. A fresh population of 80% singlet cells by

(31) Kyriakis, J. M.; Avruch, J. *Physiol. Rev.* 2001, 81, 807–869.

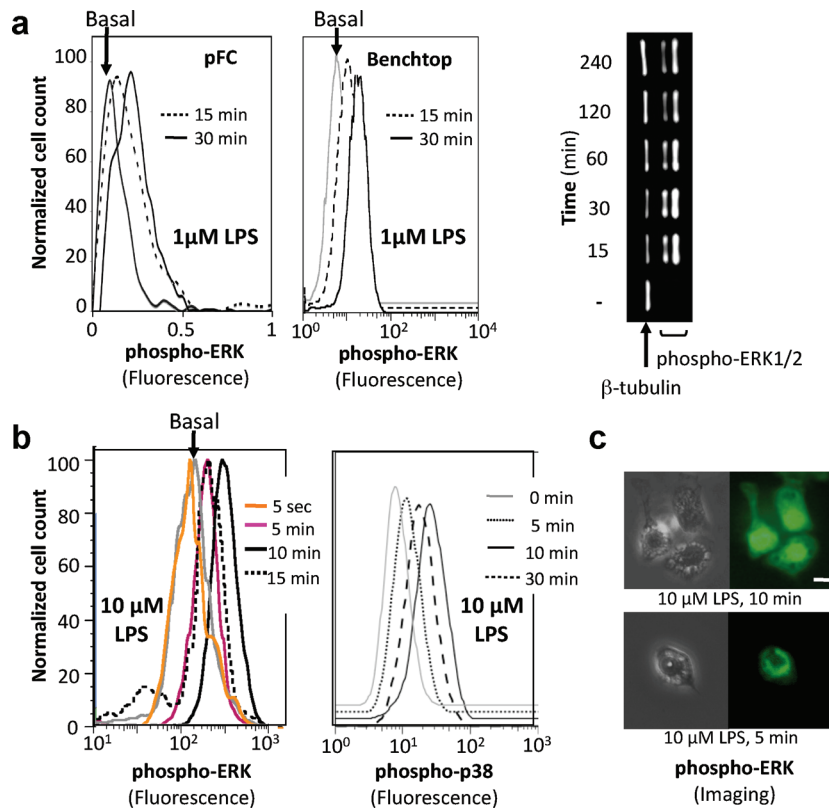


Figure 5. pFC phosphorylation assay shows time-dependent multiepitope response to *E. coli* LPS stimulation. (a) Flow cytometry reveals phosphorylation response of ERK1/2 using both conventional and integrated pFC analysis for LPS challenge ($1\text{ }\mu\text{M}$ LPS; 15 and 30 min). Peak amounts of phosphorylated ERK1/2 is detected at 30 min using both conventional and pFC analyses. Western blot analysis shows a qualitatively similar ERK1/2 phosphorylation as a function of time for a $1\text{ }\mu\text{M}$ LPS challenge. (b) Phosphorylation of ERK1/2 occurs by a 5 min postchallenge under a high *E. coli* LPS ($10\text{ }\mu\text{M}$) challenge. Phosphorylation of ERK1/2 is maximum at 10 min at this higher LPS dosage and begins to dephosphorylate by 15 min. While pFC handling allows analysis of an intracellular signaling response as early as 5 s poststimulation, significant ERK1/2 phosphorylation is not detected, as is expected. Analysis of p38 phosphorylation reveals a response to a high LPS challenge by 5 min after stimulation. Peak levels of phosphorylated p38 are detected at 10 min which proceeds to decrease by 30 min poststimulation. (c) Bright field micrographs from the spiral incubation chambers show macrophage cells, while fluorescence micrographs show the recruitment of phosphorylated ERK1/2 to the nucleus at 10 min post $10\text{ }\mu\text{M}$ LPS stimulation. Scale bar is $10\text{ }\mu\text{m}$.

flow cytometry was split and stimulated, phospho-stained, and analyzed using both the pFC platform and benchtop protocols (Figure 4b). The starting cell density (5×10^6 cells/mL) was maintained equal for both on-chip and off-chip assays. After benchtop preparation, flow cytometry side scatter vs. forward scatter identified $45 \pm 6\%$ of the cells as singlets. After pFC handling and preparation, $70 \pm 9\%$ of the cells were found to be singlets. Likewise, bright field imaging of the benchtop and pFC prepared cells qualitatively support the conclusion that more cell aggregates arise from the benchtop preparation than from pFC-assisted preparation (Figure 4c).

pFC Analysis of Toll-Like Receptor 4 Signaling. As a step toward understanding innate immune response to LPS, and more broadly to pathogens, we developed and optimized assays for phospho-profiling in murine macrophage cells (Figure 5). A suspension of macrophages (5×10^6 cells/mL) was introduced into the pFC platform, and ~ 2000 cells were localized in each of the two incubation chambers. Cells in the first chamber were stimulated with smooth *E. coli* LPS at 37°C at prescribed LPS dosages, while the second chamber was the negative control (i.e., no LPS). As a demonstration of a completely integrated workflow, the pFC platform was employed to monitor phospho-ERK1/2 using the pFC on-chip imaging and flow cytometry

capabilities. Increasing levels of phospho-ERK1/2 in response to macrophage insult with LPS ($1\text{ }\mu\text{M}$) were observed after both 15 and 30 min challenge intervals (Figure 5a). Benchtop flow cytometry and Western blot assays yielded trends similar to those observed using the pFC tool (Figure 5a). Phospho-profiling experiments conducted using the pFC tool consecutively were in agreement with the rising and falling levels of phosphorylation of intracellular proteins and yielded a peak value of phospho-ERK1/2 at the 30 min challenge ($1\text{ }\mu\text{M}$ LPS) time point with negligible day-to-day variability in the median fluorescence value (<5%). During rising phospho-ERK1/2 levels (15 min challenge), we observed a 14% day-to-day variability in the median fluorescence. The later time point (60 min challenge) exhibited decreased phospho-ERK1/2 levels, in which we observed a <5% day-to-day variability in the median fluorescence value.

To test the fluid control characteristics of the pFC platform, macrophage cells were challenged with $10\text{ }\mu\text{M}$ *E. coli* LPS for an ultrashort interval of 5 s, as well as at more conventional 5, 10, and 15 min challenge intervals. In the TLR4 signaling model examined, we did not expect nor did we observe phospho-ERK1/2

(32) Shinohara, H.; Inoue, A.; Toyama-Sorimachi, N.; Nagai, Y.; Yasuda, T.; Suzuki, H.; Horai, R.; Iwakura, Y.; Yamamoto, T.; Karasuyama, H.; Miyake, K.; Yamanashi, Y. *J. Exp. Med.* **2005**, *201*, 333–339.

after a 5 s LPS stimulation interval, as ERK1/2 phosphorylation is reported to initiate no earlier than 5 min.^{32,33} Acquisition of the 5 s data did verify our capability to assess cell response after an ultrashort challenge interval. After longer LPS stimulation, we did observe both phosphorylation and dephosphorylation of ERK1/2, as anticipated. For the pFC prepared cells, flow cytometry revealed significant increases in the levels of phosphorylated ERK1/2 and p38 at 5 and 10 min LPS exposure (Figure 5b). Dephosphorylation of these MAP kinases was observed at longer stimulation (15 and 30 min). Fluorescence imaging of macrophage cells after phospho-staining and prior to cell release for flow cytometry showed translocation of phospho-ERK1/2 into the nucleus (compare 5 and 10 min LPS-challenge, Figure 5c). The pFC analysis also revealed that phosphorylated ERK1/2 peaked earlier for the higher concentration of *E. coli* LPS (10 min for 10 μM LPS), as compared to the lower LPS concentration (30 min for 1 μM LPS) (Figure 5a, b). The pFC analysis using a unified workflow (LPS challenge through flow cytometry) allowed monitoring studies to be completed autonomously in a fraction of the time needed for similar analysis using conventional preparatory methods with flow cytometry. The pFC postinfection cell handling and analysis were completed in ~30 min, as compared to a conservative ~120 min using benchtop preparation and analysis.

DISCUSSION

Cell signaling analysis using a unified preparatory and analytical tool such as the pFC technology described in the present work offers several advantages including (i) automated workflow, including the introduction and exchange of multiple reagents (e.g., paraformaldehyde, methanol, wash buffer, antibody solution) using an electronically addressable, low volume, and rapid fluid exchange format relevant to high fidelity data set generation, (ii) reduced consumption of expensive reagents and precious samples by an order of magnitude as compared to benchtop handling, (iii) the capability to monitor early signaling events (~5 s), (iv) efficient analysis times and the associated potential for high-throughput signaling studies using a parallelized microfluidic format, and (v) improved cell handling as compared to conventional flow cytometric preparation, including the ability to readily study small cell populations with notably reduced cell clumping and losses. Here complete preparation and analysis, not including the desired varied challenge intervals, is less than 30 min. We validate the pFC analytical technology using the TLR4 mediated response of macrophage cells to LPS through phosphorylation analysis of MAP kinase proteins. Conventional flow cytometry and Western blot analyses support the assertion that the pFC tool provides a facile means for monitoring phosphorylation and dephosphorylation of key intracellular signaling proteins.

To test the capability of monitoring intracellular signaling after short LPS stimulation periods, we analyzed phospho-ERK1/2 response in macrophage cells after a burst (5 s) of LPS challenge. Stimulation periods on the order of a few seconds are difficult to implement with benchtop cell handling methods (i.e., Petri dishes, centrifuge tubes), yet the 5 s period reported here was readily achievable using convenient fluid handing enabled by microfluidic technology. The shortest stimulation duration attainable using the

pFC technology is determined by the time required for fluid exchange in the incubation chambers (i.e., volume of chamber, flushing volumetric flow rate). On the basis of the geometry of the fluidic network and the hardware used, the pFC tool could support flow rates an order of magnitude higher than the 5 s duration used in the present study. Employing such rapid fluid exchange conditions should yield an ultrashort incubation period of ~100 ms. Caution should be employed, however, as such high flow rates and short stimulation periods may not be appropriate for all systems, as is the case with phospho-ERK1/2 monitoring in the murine macrophage-LPS system currently under study. Nevertheless, signaling outside the scope of this study would potentially benefit from short-time scale monitoring. Examples include short-lived nuclear phospho-proteins (e.g., c-myc protein), rapidly changing cytoplasmic Ca²⁺ levels, aggregation of surface receptors, protein phosphorylation, and subsecond protein oscillations in platelets.^{34,35}

An important aspect of the pFC design is elimination of conventional centrifuge-based cell washing steps required for benchtop phospho-profiling. To eliminate centrifuge-based washing, the pFC approach employs microdevice-based filters for nonadherent cells and stopped flow and settling conditions for adherent cells. Although beyond the scope of the present study, the pFC approach, with reduced cell aggregation and losses, will likely appeal to the single-cell analysis of small populations such as primary and stem cells. Cell clumping, disintegration, and cell loss due to centrifugation have been reported to be major obstacles to single cell studies especially in picoeukaryotes.³⁶ Host-pathogen interaction studies requiring biohazard specialized, space-limited facilities (i.e., biosafety level 3 or 4 laboratories) could benefit from the integrated microfluidic devices demonstrated in this work. Host-pathogen studies would also benefit from the contained delivery of reagents accomplished in the completely enclosed system with no aerosol generation and minimal user exposure to risk agents used in infection studies.

The pFC approach was optimized to monitor and quantitate subcellular localization and the time-response of intracellular protein phosphorylation events key to a macrophage response to LPS infection. Analysis of intracellular phosphorylation of additional key signaling proteins, the process of phagocytosis, and the formation of surface receptor complexes is underway using the pFC platform. Further studies regarding LPS recognition by macrophage cells may contribute to the development of novel strategies for therapeutic intervention (e.g., endotoxin shock). The versatility of pFC allows for analysis of both adherent and nonadherent cell types and can be used for novel coculture assays that are otherwise not possible with existing instrumentation. The generic and versatile nature of pFC, with the capability of automation, controlled dosages, ultrashort timed incubation, and contained routing of reagents and waste, makes the pFC applicable for the exploration of a wide variety of cell biology, immunology, and cancer biology questions.

ACKNOWLEDGMENT

The authors acknowledge Dr. C. Branda, Mr. D. Throckmorton, Dr. K. Patel, Mr. H. Tran, and Dr. T. Perroud of Sandia

(33) Beinke, S.; Robinson, M. J.; Hugunin, M.; Ley, S. C. *Mol. Cell. Biol.* **2004**, 24, 9658–9667.

(34) Carty, D. J.; Spielberg, F.; Gear, A. R. L. *Blood* **1986**, 67, 1738–1743.

(35) Raha, S.; Jones, G. D.; Gear, A. R. L. *Biochem. J.* **1993**, 292, 643–646.

National Laboratories for providing materials and for helpful discussions. Funding was provided by the Sandia National Laboratories Internal Laboratory Directed Research and Development Office, through the Microscale Immune Studies Laboratory “Grand Challenge” project. Sandia is a multiprogram laboratory operated by Sandia Corp., a Lockheed Martin Co., for the U.S. Department of Energy under Contract DE-AC04-94AL85000.

(36) Biegala, I. C.; Not, F.; Vaulot, D.; Simon, N. *Appl. Environ. Microbiol.* 2003, 69, 5519–5529.

SUPPORTING INFORMATION AVAILABLE

Additional information as noted in text. This material is available free of charge via the Internet at <http://pubs.acs.org>.

Received for review November 14, 2008. Accepted February 5, 2009.

AC8024224